International Journal of Pharmaceutical and Bio-Medical Science

ISSN(print): 2767-827X, ISSN(online): 2767-830X

Volume 01 Issue 08 November 2021

Page No: 134-143

DOI: https://doi.org/10.47191/ijpbms/v1-i8-03, Impact Factor: 5.374

Comparison of PSF and Non PSF BLOB based reconstructed image in Time-of-Flight PET/CT

Manish Kumar Vishwakarma[1], Dr. Shashwat Verma[2], Dr. Satyawati Deswal[3]

[1]Dr. Ram Manohar Lohia Institute of Medical Sciences, Lucknow

[2,3]Dept of Nuclear Medicine Dr. RMLIMS Lucknow

ABSTRACT

Hybrid PET/CT imaging with the use of ^{18}F FDG is a widely used imaging technique with major indications in oncology for staging, re-staging and monitoring response to therapy. There is a major issue of partial volume effect in PET images which affects image quality as well as quantitative accuracy in small lesions. Multiple attempts have been made to resolve these issues. The aim of our study was to look into impact of Point-spread-function (PSF) on reconstructed attenuation corrected (AC) images of PET/CT and to find out best combination of the number of PSF iterations with regularization level while applying PSF.

Methods

We performed phantom study before performing patient study with similar algorithm on a time of flight (TOF) PET/CT system. We used NEMA IEC body phantom filled with appropriate activity in spheres and background area. After acquisition, data reconstructed three times, non PSF, 2PSF and 4PSF. We measured noise, CRC and SNR in all 3 sets of reconstructed phantom image. We selected 96 patients for our study and acquisition was performed similar to phantom study followed by data reconstruction. In all three sets of data reconstruction we measured SUVmax, SUVmean and lesion volume for both phantom and patient study. All quantitative data and lesion detectability in 2PSF and 4PSF images were visually assessed by two nuclear medicine physicians.

Results

The measured background noise, CRCmax and CRCmean were significantly increased in 2PSF and 4PSF images as compared to non PSF. The SNRmax relatively increased in 2PSF as compared to non PSF and decreased in 4PSF as compared to 2PSF for lesions <2cm. In lesions >2cm SNRmax was not much significantly increased as compared to small lesions (<2cm). The SUVmax was increased in 2PSF & 4PSF as compare to non PSF while in SUVmean, values were not significantly increased as compared to SUVmax.

Conclusion

2PSF iterations combined with the 6 regularization level reconstructed PET image play a significant role in the accuracy of the SUVmax determination. SUVmean tends to be more accurate at relatively higher PSF iteration (4PSF) with smoothing levels. It gives acceptable noise and good image quality which leads to improved small lesion detection and well defined margin of the lesion.

ARTICLE DETAILS

Published On:
15 November 2021

Available on:
https://ijpbms.com/

KEY WORDS: PSFR, PSFTOF PET/CTR, TOF PET/CTSUV, SUVCRC, CRCSNR

INTRODUCTION

Positron emission tomography (PET) is a tomographic technique that computes the three-dimensional distribution of radioactivity based on the annihilation photons that are emitted by positron emitter labelled radiotracers. PET allows non-invasive quantitative assessment of biochemical and functional processes. The most commonly used tracer at present is the glucose analogue ^{18}F-fluoro-de-oxy-glucose

(^{18}F-FDG). ^{18}F-FDG accumulation in tissue is proportional to the amount of glucose utilization. Increased consumption of glucose is a characteristic of most cancers and is in part related to over-expression of the GLUT-1 glucose transporters and increased hexokinase activity *(1)*.

First PET systems were designed in the mid-1970s. One of the most important progresses in PET was the introduction of time of flight (TOF) PET systems. The concept of TOF means simply that for each annihilation event, we note the precise time that each of the coincident photons is detected and then we calculate the difference*(2)*. The advantages of the use of TOF PET relates to noise reduction and a higher accuracy in the reconstructed image.

Image quality improvement in PET images is under continued progress and development of PET system manufacturers. Algorithm of reconstruction is the most important part to improve image quality. Recently, the information provided by the point-spread function (PSF) and TOF has been expected to improve the spatial resolution and signal-to-noise ratio (SNR) of PET images. Several manufacturers have introduced TOF and PSF algorithms that improve SNR in conjunction with iterative reconstruction (IR) including the most commonly used ordered subsets expectation maximum (OSEM) algorithms.

When a photon strikes a crystal, it travels a distance before being converted into light. This depth-of-interaction is usually not known. Therefore, if the photon comes from the center of the field-of-view (FOV), the line of response (LOR) is likely to be correctly localized in the crystal within the block. Further away from the center of the FOV, less likely the LOR will be calculated correctly because photon will hit the crystal on an angle and continue travelling to another crystal before it lights up, causing the parallax error. PSF aims to minimize this blurring effect throughout the entire FOV. By minimizing the spillover of counts from one voxel into adjacent voxels, image contrast is improved and image noise is better controlled. Newer-generation clinical PET/CT are equipped with PSF reconstruction algorithms and are more sensitive for small-volume lesion *(3)*.

The PSF describes response of an imaging machine to a point object. A more general term for the PSF is a system's impulse response. The PSF could be thought as the extended blob in an image. PSF reconstruction produces images with improved spatial resolution, reduced partial volume effect and ultimately increased activity concentration (Bq/mL) or standardized uptake value (SUV) in small lesions. These lesions are easily detected and characterized. There is a growing interest for using PET in the prediction and evaluation of early responses to treatment, such as chemotherapy, radiotherapy and local ablative therapy, e.g., of liver metastases, in order to identify non-responders as soon as possible to optimize their treatment strategy. These benefits have been demonstrated as higher recovery coefficients (RCs) in NEMA IEC phantom studies and improved lesion detection in patient studies *(4)*.

High-density bismuth germinate (BGO) crystal has been widely used to pursue a high sensitivity system, although its slow decay time has not been suitable for the TOF strategy. The development of lutetium oxy-orthosilicate(LSO) and lutetium yttrium oxy-orthosilicate (LYSO) has reawakened interest in TOF PET*(3)*, because these scintillators have both a fast decay time and high density with good stopping power for 511-keV photons. The ability to measure the difference between the arrival times of a pair of photons originating from positron annihilation improves the image SNR. The level of improvement depends upon the extent and distribution of the positron activity and the timing resolution of the PET scanner.

The simple quantification methods were proposed to take into account in clinical PET acquisition. The most widely used semi quantitative method is the SUV.

SUV = Tissue FDG Uptake (Activity concentration Bq/mL) x Body weight / Injected Activity (Bq).

The major objective of this investigation was to assess the image quality of TOF PET image data in non PSF and after applying 2 PSF iteration;6 regularization levels and 4 PSF iteration;6 regularization level acquired with 1-minute time frame. Quantitative and qualitative analysis was done using data of 96 patients. We evaluated its effect on several parameters: SUV_{max}& SUV_{mean}, SNR_{max} & SNR_{mean} and image quality for ^{18}F-FDG PET/CT scan in cancer patients.

MATERIALS AND METHODS

PET/CT System

We had imaged all the patients on PHILIPS INGENUITY TF PET/CT (Philips Medical Systems) with 128 slice CT hybrid system which comprised pixilated 28,336 LYSO crystals arranged in an Anger-logic detector design to achieve uniform light spread in the detector. Astonish TF technology is combined with an overlapping spherically symmetric volume binary large object (blob) basis function that leads not only to substantial suppression of the image noise but also to preservation of the resolution compared to conventional cubic voxels *(5)*. This blob approach allows Philips scanners to achieve better contrast-to-noise performance over voxel reconstruction *(6)*. PET is equipped with 44 rings of pixellar type LYSO- detector (diameter of 90cm) with axial 18cm detector coverage. System sensitivity is more than19400 cps/MBq(in centre) and timing resolution of 540 picoseconds. All the data was acquiredin 3-D mode and stored in list mode format with TOF reconstruction for better localization accuracy. PET/CT system uses excellent contrast and image resolution to help make details, like small lesions visible. The energy resolution is 12% and the accepted energy window 440 KeV to 665 KeV. Our PET/CT system had some similar construction to the Philips Gemini TF PET/ CT*(7)*.Images are reconstructed using a TOF, list-mode,

blob-based, TOF three-dimensional row-action maximum likelihood algorithm (3D-RAMLA) *(8)*.

PHANTOM STUDY

A NEMA phantom which represents standard body size simulating patients with a 60 kg body weight and 84 cm waist was used in our study*(9)*. A NEMA IEC BODY PHANTOM of model ECT/IEC-BODY/P consists of body phantom (interior length of 18 cm), lung insert and an insert with six spheres (10, 13, 17, 22, 28 and 37mm inner diameter. The six spheres are filled with radioactivity to represent hot lesions and the background volume is filled with low-level uniform radioactivity. The central lung insert was filled with moulded expanded polystyrene beads. The large background compartment (Torso) and the 6 spheres were filled with a solution of ^{18}F-FDG in a concentration of10.36 KBq/mL and 57.72 KBq/mL respectively, resulting in a sphere to background ratio of approx 6:1. A 4-mm pixel size was used in all PET studies in order to lower the noise level. The intrinsic noise reduction in TOF images allows higher spatial resolution to be utilized.

In all six spheres, we determined the maximum and mean ^{18}F-FDG concentration (KBq/mL) in three reconstructed image sets. Furthermore, background measurements were performed using region of interest (ROI) on the NEMA phantom. We performed background measurements on the most central axial slice, at least 15 mm away from the phantom edge and the phantom spheres to prevent influence of the partial-volume effect. The mean ^{18}F-FDG concentration and standard deviation (SD) in the ROI were determined for the background. Using following equation, we calculated the noise in the phantom background compartment.

Noise = SD_{Bkg} / C_{Bkg})

Where C_{Bkg}-18F-FDG concentration background

SD_{Bkg}- SD of the 18F-FDG concentration background

Contrast recovery coefficients (CRC) is defined as the ratio between the measured (maximum or mean) ^{18}F-FDG concentration in the images (C measured) and the true ^{18}F-FDG concentration in the sphere (Ctrue). For each sphere, we determined the CRCmax and CRCmean. (Table-1)

CRC = C measured / Ctrue

Phantom spheres Ctrue was 57.72 kBq/mL at 8.58 am, and 3841 Bq/mL at 4.07 pm.

We also calculated the SNRmax and SNRmean using following equation-

SNR = Cmeasured/SD_{Bkg}

DATA RECONSTRUCTION

PET data were reconstructed three times. First reconstruction was done by default settings and called as Non PSF images. Second reconstruction was done by using 2PSF iteration and 6regularization level. Third reconstruction was done by using 4PSF iteration and 6 regularization level. All three sets images were reconstructed using a default 3-D TOF-OSEM and 144x144 matrix with a voxel size of 4x4x4mm. To compensate for detector blurring, a blob-based reconstruction was applied. These spherical symmetric image elements (blobs) were used instead of voxels for image representation *(10)*. All reconstruction parameters were default settings recommended by the manufacturer.

PATIENT AND LESIONS

All patients signed a written informed consent form, and this study was approved by institutional ethical committee. Study duration was 6 months. Ninety six patients (45 males, 51 female) with advanced cancer who were referred for a whole-body ^{18}F-FDG PET/CT examination for cancer staging and treatment follow up were included in this study. The mean age, height and weight for males were 49.29±10.2 years, 165.2±5.1cm and 60.8±9.4Kg respectively. For females the mean age, height and weight were 49.55±13.8years, 152.9±7.5cm and 53.8±10.9Kg respectively. We had grouped the lesions in two categories based on lesion diameter- Lesion A and Lesion B. The Lesion A were 69 (mean size 13.04±3mm) and Lesion B were 27 (mean size 36 ±12mm).

We had determined the lesion volume by drawing a 3-D ROI, based on iso-contours at 50% of the maximum pixel value in non PSF, 2PSF & 4PSF reconstructed PET images. Lesion A was <2cm (but not <0.9 mm) and lesion B was >2 cm. Lesions were considered as ^{18}F-FDG PET positive when there was an increased uptake (visually assessed). A maximum 3 lesions per patient were included in the study. If any patient had many small lesions, then in these cases, the smallest lesions were selected in both lesion categories. Lesions were located in mediastinum (26), lung (17), breast (03), cervical region (05), axillary region (11), thyroid (05), brain (03), inguinal (2) and other miscellaneous regions.

For each lesion, we measured the SUVmax, SUVmean, SNRmax and SNRmean and noise. We took background measurements on the mediastinal blood poolby drawing an ROI of approximately 400 mm^2. For background, we calculated the SUVmax and SUVmean.

For all parameters, we determined the relative changes in all sets of reconstructed images.

For qualitative visual analysis, 2 experienced nuclear medicine physicians, who were unaware of the study purpose, performed analysis of the changes in all sets of reconstructed image.

For the all selected lesions, both nuclear medicine physicians had to rank their preference based on contrast and sharpness of the lesion and also for the diagnostic confidence. Image quality was scored on a 3-point Likert scale.

^{18}F-FDG PET/CT Protocol

Patients were asked to fast for at least 6 hours before the injection. ^{18}F-FDG was injected intravenously (with 3.7-5.55 MBq/kg) according to EANM guidelines for tumor imaging*(4)*. Blood glucose level was checked before the

injection. Patient mean blood glucose level was 115±17mg/dL. The mean duration of the uptake phase was 86 min (45-90 min).

Vertex to the mid-thigh area was covered in the whole-body PET/CT scan. Approx 10 different bed positions were necessary in most cases. First a low dose helical CT scan for attenuation correction was acquired during shallow breathing (using iDose4), 110 mAs, 120 KVp, pitch 0.8 and rotation0.4s with the arms over the head. Iodinated intravenous contrast was administered according to body weight at 1.6 mL/sec flow rate, if required. CT scanning was started after 50 second of contrast administration. Immediately thereafter whole-body ^{18}F-FDG PET/CT scans using 1-minute acquisition time per bed position was obtained for each patient. PSF were applied after acquisition and images were reconstructed.

IMAGE ANALYSIS

Images were interpreted at a workstation (IntelliSpace Portal 6; Philips Healthcare) equipped with fusion software that enables the display of CT, PET and PET-CT images. All PET/CT images were read by two certified nuclear medicine physicians.

RESULT

Phantom study

The acquisition was performed on NEMA IEC body phantom and images were reconstructed using three different algorithmsi.e. non PSF, 2PSF iteration; 6 regularization level and 4PSF iteration; 6 regularization level. SUVmax, SUVmean and volume (mm^3) of all 6 hot spheres were measured(Table-1 and Figure 1).The mean standard error (SE) of SUVmean for all sizes of hot spheres was 4.3%, 5.6%, 4.9% and mean SE of SUVmax for all sizes of hot spheres was 6.4%, 8.2 %, 9.3% in non PSF, 2PSF and 4PSF reconstruction respectively. The background noise level was measured in the phantom and was 6.60% in non PSF, 7.60% in 2 PSFand 9.40% in 4 PSF images. The impact of PSF algorithm on CRCmax, CRCmean, SNR max and SNR mean is summarized in the Table-2. All parameters were increased in 2PSF and 4PSF image as compared to non PSF images. In small lesions (<20mm), the relative increase in CRC max, CRC mean were highest in 4PSF but relative increase in SNRmax and SNR mean were the highest in 2PSF. The CRCmax relatively increased by 41 ±9% in 2PSF and 65±12% in 4PSF for hot lesion size 10mm, 13mm,17mm i.e. lesion category A. The CRC max relatively increased by 25 ±8% in 2PSF and 34±10% in 4PSF for hot lesion size 22mm, 28mm, 37mmi.e. Lesion category B (Fig-2A). The CRCmean relatively increased by 35±11% in 2PSF and 49±8% in 4PSF for hot lesion category A. The CRCmean relatively increased by 19±06% in 2PSF and 26±10% in 4PSF for lesion category B.The lesions showed measurement error by 26±4% in non PSF, 3±11% in 2PSF and 6±9% in 4PSF for hot lesion category A(Fig-2 B). The 4 PSF reconstructed image showed the measured lesion size higher, compared to non PSF. The lesions of size more than 20mm (category B) showed measurement error of 10 ±7% in non PSF, 3±5% in 2PSF and 3±6% in 4PSF.The SNRmax relatively increased by 30 ±12% in 2PSF and 22±10% in 4PSF for hot lesion category A as compared to non PSF. The SNRmax relatively increased by 10 ±7% in 2PSF and5±7% in 4PSF for hot lesion category B. The 4 PSF reconstructed image showed the less SNRmax as compared to 2PSF. According to these values we should not use more PSF iteration which decreased the SNR further.

The P value for SUVmax was 0.028 (significant<0.05) when comparing SUV max of 2PSF and 4PSF images with Non PSF images (SUVmax 4PSF>2PSF>non PSF)

The P value for CRCmax was 0.028 (significant<0.05) when comparing CRC max of 2PSF and 4PSF images with non PSF images (CRCmax 4PSF>2PSF>non PSF)

The P value for SNRmax was 0.028 (significant<0.05) when comparing 2PSF SNRmax with non PSF images. The SNRmax in 4PSF was less than 2PSF SNRmax but more that non PSF SNRmax (SNRmax 2PSF>4PSF>non PSF) (Fig-2 C).

The P values for SUVmean was 0.028 (<0.05) when comparing 2PSF with non PSFand it was 0.046 (<0.05)when comparing 4PSF with non PSF.

The P values for SNRmean was 0.046 (<0.05) when comparing 2PSF with non PSF and it was 0.116 (>0.05) when comparing 4PSF with non PSF. The P values for CRCmean were 0.028 (<0.05) when comparing 2PSF with non PSF and it was 0.207 (>0.05) when comparing 4PSF with non PSF.

There was no significant difference found in SNRmean or in CRCmean when comparing 4PSF with non PSF.

LESION VOLUME- The relative change in the lesion volumes on PET images between the non PSF, 2PSF was 31±4% and between non PSF, 4PSF image was 39±11%, for less than 2 cm lesion (lesion category A). The relative change in the lesion volumes on PET images between the non PSF, 2PSF was21±18% and between non PSF, 4PSF images was 25±18%, for more than 2 cm lesion (lesion category B). Lesion volume was significantly decreased in PSF based images as compared to non PSF images.(Fig-2D)

Patients Study

Lesion SUV value-P value was<0.01 while comparing SUVmax of non PSF, 2PSF& 4PSF images i.e. SUV max 4 PSF>SUV max 2 PSF > SUV max non PSF.

The mean difference in relative change of non PSF and 2PSF SUVmax for lesion A and lesion B was 39±11% and 36±14% respectively. The mean difference in relative change of non PSF and 4PSF SUVmax for lesion A and lesion B was 59±18% and 52±19% respectively.

P value was <0.01 while comparing SUVmean of non PSF, 2PSF& 4PSF images i.e. SUV mean 4 PSF>SUV mean 2 PSF > SUV mean non PSF.

The mean difference in relative change of non PSF and 2 PSF SUVmean for lesion A and lesion B was 30±25% and 21±23% respectively. The mean difference in relative change of non PSF and 4PSF SUVmean for lesion A and lesion Bwas 47±34% and 24±35% respectively.

Lesion SNR- The P value was<0.01(significant) while comparing SNRmax of non PSF and 2PSF imagei.e. 2PSF SNRmax was greater than non PSF SNRmax for all category lesions.

The P value was <0.881(not significant) while comparing SNR max of 2PSF and4 PSF image i.e. 2PSF SNRmax was greater than 4PSF SNRmax for all category lesions.

There was significant difference (P<0.01) between SNRmean of non PSF and 2PSF reconstructed image for all category lesions.

There is no significant difference (P<0.359) between SNR mean of 2PSF and 4PSF reconstructed image for all category lesions.

The Fig. 3 shows the images of patient with various PSF algorithms. It was very clear that the image quality was most appropriate with significant difference in SNR max and SNR mean of non PSF and 2 PSF images.

Lesion Volume - For the Lesion group A, there is a significant difference at 1% level between lesion volume of non PSF and PSF image as on Wilcoxon signed ranks test based on positive ranks. Positive ranks were less than negative ranks i.e. non PSF lesion volume was greater than 2PSF lesion volume. There was significant difference at 1% level between lesion volume of 2PSF and 4PSF image. Positive ranks were less than Negative ranks i.e. 2PSF lesion volume was greater than 4PSF lesion volume. P values were <0.05(significant).

For the Lesion group B, there was significant difference at 1% level between lesion volume of 2PSF and non PSF image as on Wilcoxon signed ranks test based on positive ranks. Positive ranks were less than Negative ranks i.e. non PSF lesion volume was greater than 2PSF lesion volume. P value was <0.019(significant). There was significant difference at 1% level between lesion volume of 4PSF and 2PSF image. Positive ranks were less than Negative ranks i.e. 2PSF lesion volume was still greater than 4PSF lesion volume although P value was <0.171 (not significant).

DISCUSSION

We evaluated the effect of PSF on image quality and determined the parameter for reconstruction by phantom study which was followed by patient study. Our study reveals that small lesions detection on a TOF PET/CT system can be improved by using PSF based reconstructions. Our nuclear medicine physicians preferred the PSF based ^{18}F-FDG PET reconstructed images to identify lesions less than 2cm easily. PSF based images increases diagnostic confidence.

The mean standard error (SE) of SUVmean was 4.3%, 5.6%, 4.9% in non PSF, 2PSF, 4PSF reconstruction subsequently. SUVmean should be considered while applying more number of PSF iteration.

The background noise level was 6.60%, 7.60% and 9.40% non PSF, 2PSF, 4PSF reconstructions subsequently. We inferred that with increasing PSF, the lesion size and image acceptability was most appropriate for 2PSF data.

The most important elements in quantitative PET imaging is Partial volume effect. For improving the quantitative accuracy, many attempts have been made. Partial volume can be quantitatively corrected using simple measurements of objects at different physical sizes that extends from few millimeters up to approx three times of the spatial resolution of the system (2-3 FWHM). The Ingenuity TF PET/CT employs blob-based list-mode TOF reconstruction followed by PSF-based ordered subsets expectation maximization (OSEM) de-convolution resolution recovery. De-convolution approach could potentially improve the quantitative measurements of acquired PET data but at increased noise levels.

Previous studies reported that using of PSF, can lead to accurate quantitative analysis, with some SUV overestimation (11). Thus, we reconstructed image in different reconstruction parameters to reach the acceptable image quality in oncology patients undergoing PET/CT imaging. In general the results of our study are consistent with previous hybrid PET studies *(5, 12 &13)* that iterative PET reconstruction can improve the activity recovery and image noise.

According to our phantom study CRC mean/max and SNR mean/max was measured and found increased in 2 PSF and 4 PSF reconstructed image as compared to non PSF images. In the phantom study we found that lesion volume was exceeded in the non PSF image, while after applying the PSF, lesion margins became well defined and lesion volume improved. An increase in the number of PSF iterations led to a rise in the frequency and a decrease in the wavelength of the radioactivity profile. In the 4PSF images, lesion volume further improved but image quality deteriorated and false positive results could be seen. However, Yuji Tsutsui et al (14) had told in their study that an increase in the PSF iterations resulted in narrow edge artifacts. They examined edge artifacts in phantom which appeared as an overestimation of the RCmax (Recovery Coefficient maximum). This overestimation was dependent on the pixel size, number of iterations, and FWHM of Gaussian filter. In our study, we have used smoothing regularization level with PSF and used 4mm voxel size to reduce such type of edge artifact. Edge enhancement of the small lesion (<2cm) could be easily diagnosed in patient and improves the visibility of

the lesion. An overestimation of CRCmax in phantom study up to 33% & 48% was found respectively, in 2 PSF and 4 PSF reconstructions.

Our results are consistent with previous study *(5)* which stated that SUVmean was maintained stable for smallest spheres, through few combinations of PSF & regularization level. The higher contrast ratio requires less number of PSF iterations because it reduced image quality. In our phantom study, SUVmean also increased significantly after increasing the PSF iteration but we had fixed 6 regularization level. We had used 2PSF, 6 regularization level & 4PSF, 6 regularization levels for both phantom and patient, having lesions less than 2 & more than 2 cm. Image qualities was best at 2PSF, 6 regularization.

The SUVmax is a popular quantification parameter which is used in 91% of diagnostic reports. In our study we had measured both SUVmax and SUVmean after applying PSF and 6 regularization level (default setting), without applying further smoothing filters. The SUVmax was significantly increased when applying and increasing PSF iterations. SUVmean was not much increased as compare to SUVmax. In previous study *(15, 16)* SUVmax and SUVmean were also increased significantly in clinical studies.

In our study, we have used smoothing regularization level with PSF as Gaussian filters were unavailable in our equipment and used 4mm voxel size to reduce edge artifact. Edge enhancement of the small lesion (<2cm) could be easily diagnosed in patients and improves visibility of lesion. An overestimation of CRCmax in phantom study was found in 2PSF and 4PSF reconstructions.

In the previous study *(9)* SNR max/mean was improved using PSF and TOF information. The improvement of spatial resolution by PSF is considered to lead to an increase in the SNR. The SNR also improved in our both phantom as well as in clinical studies. In the 4PSF reconstructions, there are more chances of false positive result due to increased SNR and SUV. We should prefer the 2PSF to avoid false positive results.

There were few limitations in our study like we had fixed regularization level by default and increased only PSF while regularization level also improves the image quality. Also, were constructed image using only 4mm voxel size while other voxel sizes could also be explored.

CONCLUSION

On the basis of our study, 2PSF iterations combined with the 6 regularization (smoothing) level reconstructed PET image plays a significant role in the accuracy of the SUVmax and SUV mean determination. SUVmean tends to be more accurate at relatively higher PSF iteration (4PSF) with smoothing levels. It gives acceptable noise and good image quality which leads to improved small lesion detection and well defined margin of the lesion. Physicians mostly preferred ^{18}F-FDG PET images reconstructed with 2PSF iteration and 6 regularization level than non PSF and 4PSF iteration and 6 regularization level. 4PSF based reconstruction increases the SUV and SNR for small lesions as well as for disease-free nodes, which creates difficulty in the interpretation and leads to higher rate of false-positive findings. Physician must be informed while applying PSF to avoid mis- interpretation and comparison with previous studies which were reconstructed with same algorithm.

REFERENCES

I. Boellaard R, Mike J. O' Doherty et al. FDG PET and PET/CT: EANM procedure guidelines for tumour PET imaging: version 1.0. Eur. J. Nucl. Med. Mol. Imaging. 2010; 37:181–200.

II. NEMA. NEMA Standards Publication NU2–2007: performance measurements of positron emission tomography. Rosslyn, VA: National Electrical Manufacturers Association; 2007.

III. Panin VY, Kehren F, Michel C, Casey M. Fully 3-D PET reconstruction with system matrix derived from point source measurements. IEEE Trans Med Imaging. 2006; 25(7):907-21.

IV. Munk O. L, Tolbodand L. P, Hansen S. B, et al. Point-spread function reconstructed PET images of sub-centimeter lesions are not quantitative. Eur. J. Nuc Med Mol Imaging Phys. 2017, Dec; 4(1):5.

V. Akamatsu G, Uba K, Taniguchi T, Mitsumoto K, Narisue A, Tsutsui Y, et al. Impact of Time-of-Flight PET/CT with a large axial field of view for reducing whole-body acquisition time. J Nucl Med. 2014; 42:101–104.

VI. Taniguchi T, Akamatsu G, et al. Improvement in PET/CT image quality in overweight patients with PSF and TOF. Ann Nucl Med. 2015; 29:71–77.

VII. Surti S, Kuhn A et al. Performance of Philips Gemini TF PET/CT scanner with special consideration for its time-of-flight imaging capabilities. J Nucl Med. 2007; 48:471–480.

VIII. Kolthammer J A, Grover A et al. Performance evaluation of the Ingenuity TF PET/CT scanner with a focus on high count-rate conditions. Phys Med Biol. 2014; 59:3843–3859.

IX. Akamatsu G, Mitsumoto K, Taniguchi T, Tsutsui Y, Baba S, Sasaki M. Influences of point-spread function and time-of-flight reconstructions on standardized uptake value of lymph node metastases in FDG-PET. Eur J Radiol. 2014;83:226–30

X. Lanson C, Desmonts C, Quak E, Gervais R, Do P, Dubos-Arvis C, et al. Harmonizing SUVs in multicentre trials when using different generation PET systems: prospective validation in non-small cell lung cancer patients. Eur J Nucl Med Mol Imaging. 2013;40(7):985-96.

XI. Prieto E, Penuelas I, et al. Impact of time-of-flight and point-spread-function in SUV quantification for oncological PET. Clin Nucl Med. 2013; 38(2):103-9.

XII. Sharipour R, Ghafarian P, et al. Impact of Time-of-Flight and Point-Spread-Function for Respiratory Artifact Reduction in PET/CT Imaging: Focus on Standardized Uptake Value. Tanaffos. 2017; 16(2):127-135.

XIII. Aklan B, Oehmigen M, Beiderwellen K, Ruhlmann M, Paulus DH, Jakoby BW, et al. Impact of point-spread function (PSF) modeling on PET image quality in integrated PET/MR hybrid imaging. J Nucl Med. 2016; 57(1):78-84.

XIV. Tsutsui Y, Awamoto S, et al. Edge Artifacts in Point Spread Function-based PET Reconstruction in Relation to Object Size and Reconstruction Parameters. Asia Ocean J Nucl Med Biol. 2017; 5(2):134-143.

XV. Armstrong IS, Kelly MD, Williams HA, Matthews JC. Impact of point spread function modelling and time of flight on FDG uptake measurements in lung lesions using alternative filtering strategies. Eur J Nuc Med Mol Imaging Phys. 2014;1(1):99-116.

XVI. Andersen F. L, Klausen T. L, Loft A, Beyer T, Holm S. Clinical evaluation of PET image reconstruction using a spatial resolution model. Eur J Radiol. 2013; 82(5):862-9.

Table: - 1 SUVmax, SUVmean Volume for 6 spheres in NEMA Phantom and background in Non PSF, 2 PSF and 4 PSF Reconstructions

	Non PSF			**PSF 2 Iteration**			**PSF 4 Iteration**		
Size	**SUVmax**	**SUVmean**	**Volume**	**SUVmax**	**SUVmean**	**Volume**	**SUVmax**	**SUVmean**	**Volume**
10	**2.72**	**1.62**	**1728**	**3.65**	**2.01**	**1216**	**4.29**	**2.14**	**832**
13	**3.17**	**2.26**	**2432**	**5.12**	**3.12**	**1536**	**5.91**	**3.43**	**1472**
17	**6.16**	**4.11**	**1856**	**9.32**	**5.94**	**1344**	**11.06**	**2.78**	**7040**
22	**5.57**	**3.54**	**6336**	**7.53**	**4.48**	**4992**	**8.14**	**4.87**	**4736**
28	**5.77**	**3.94**	**11264**	**7.04**	**4.71**	**9728**	**7.33**	**4.86**	**9472**
37	**6.31**	**4.12**	**28992**	**7.61**	**4.66**	**23424**	**8.24**	**4.86**	**24512**
Bkg	**1.26**	**1.06**	-	**1.24**	**1.05**	-	**1.35**	**1.06**	-

Table: - 2. CRCmax, CRCmean, SNRmax and SNRmean of 6 Phantom Spheres for non PSF, 2PSF & 4 PSF reconstruction

		10mm	13mm	17mm	22mm	28mm	37mm
Non PSF	CRCmax	0.47	0.64	1.06	0.96	0.99	1.09
	CRCmean	0.28	0.39	0.71	0.61	0.68	0.71
	SNRmax	38.86	45.29	88.00	79.57	82.43	90.14
	SNRmean	23.14	32.29	58.71	50.57	56.29	58.86
PSF 2 Iteration 6 Regularisation	CRCmax	0.63	0.88	1.61	1.30	1.21	1.31
	CRCmean	0.34	0.54	1.02	0.77	0.81	0.80
	SNRmax	45	64	116	94	88	95
	SNRmean	25	39	74	56	59	58
PSF 4 Iteration 6 Regularisation	CRCmax	0.74	1.02	1.91	1.40	1.26	1.42
	CRCmean	0.64	0.59	0.48	0.84	0.84	0.84
	SNRmax	42.90	59.10	110.60	81.40	73.30	82.40
	SNRmean	21.40	34.30	27.80	48.70	48.60	48.60

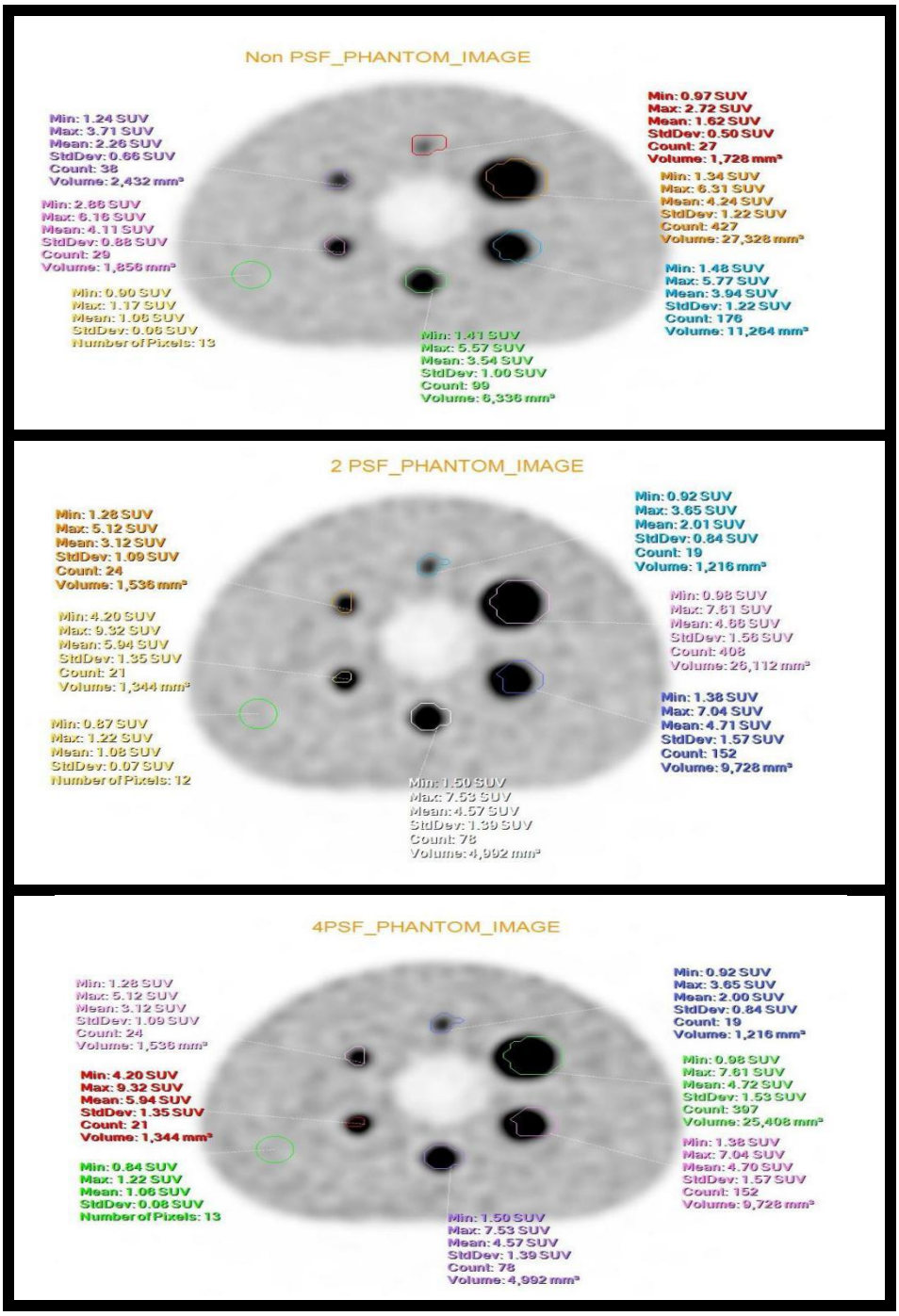

Fig. 1: PET image of NEMA phantom. Top row- Without PSF. Middle row- With 2 PSF; 6 regularization. Bottom row- With 4 PSF; 6 regularization

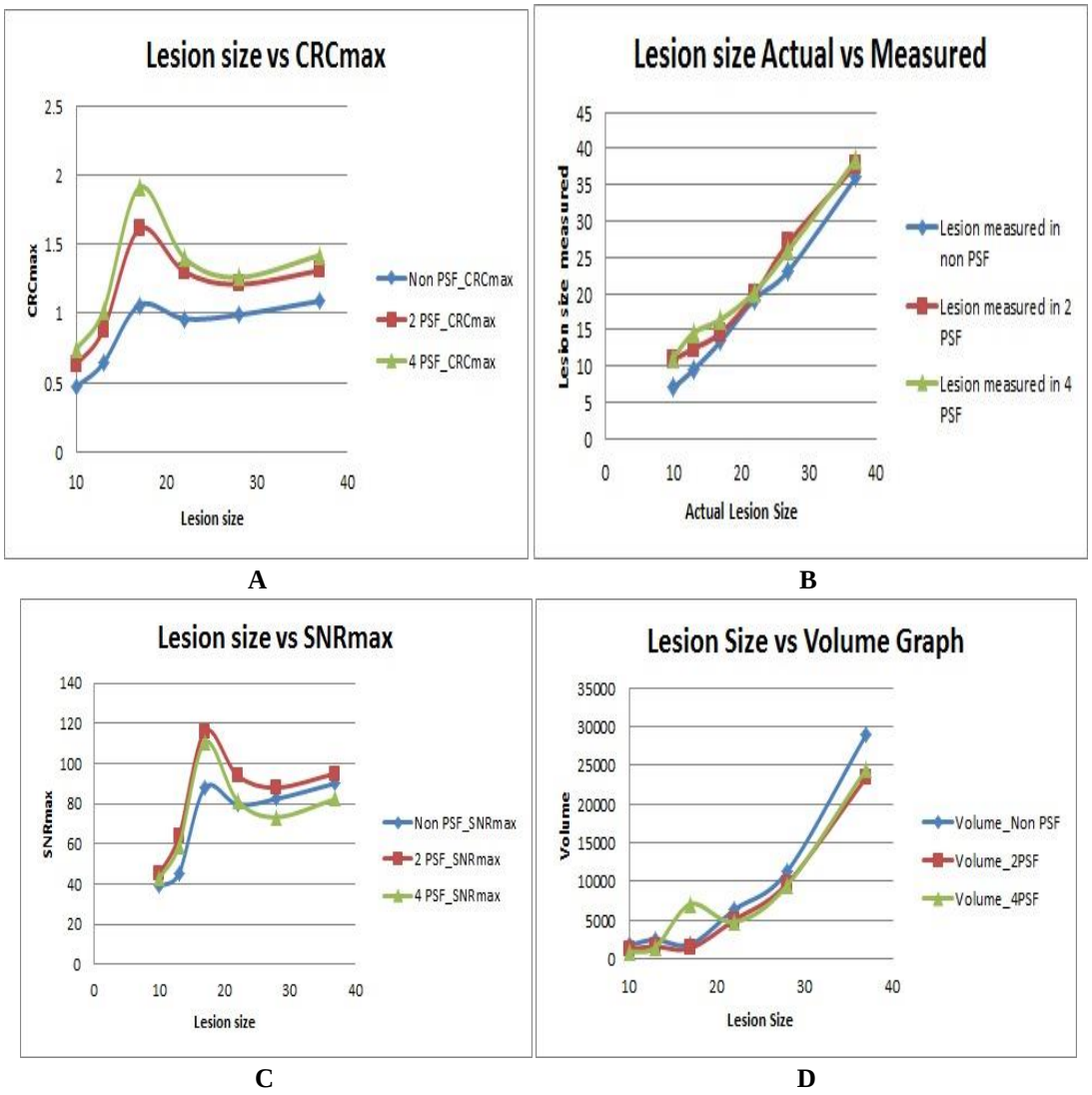

Fig-2. A: Graph for CRC max vs lesion size in non PSF, 2PSF & 4PSF. The graph shows 4PSF CRC max increased as compared to 2 PSF & non PSF. B: Graph for measured Lesion size vs Actual lesion size in non PSF, 2PSF & 4PSF. The graph shows non PSF lesion volume increased as compared to 2 PSF & 4 PSF lesion volumes. C: Graph for SNR max vs Lesion volume graph in non PSF, 2PSF & 4PSF. The graph shows 2PSF SNR max is increased as compared to 4PSF & non PSF. D: Graph for Lesion volume vs lesion size in non PSF, 2PSF & 4PSF. The graph shows non PSF lesion volume increased as compared to 2 PSF & 4 PSF lesion volumes.

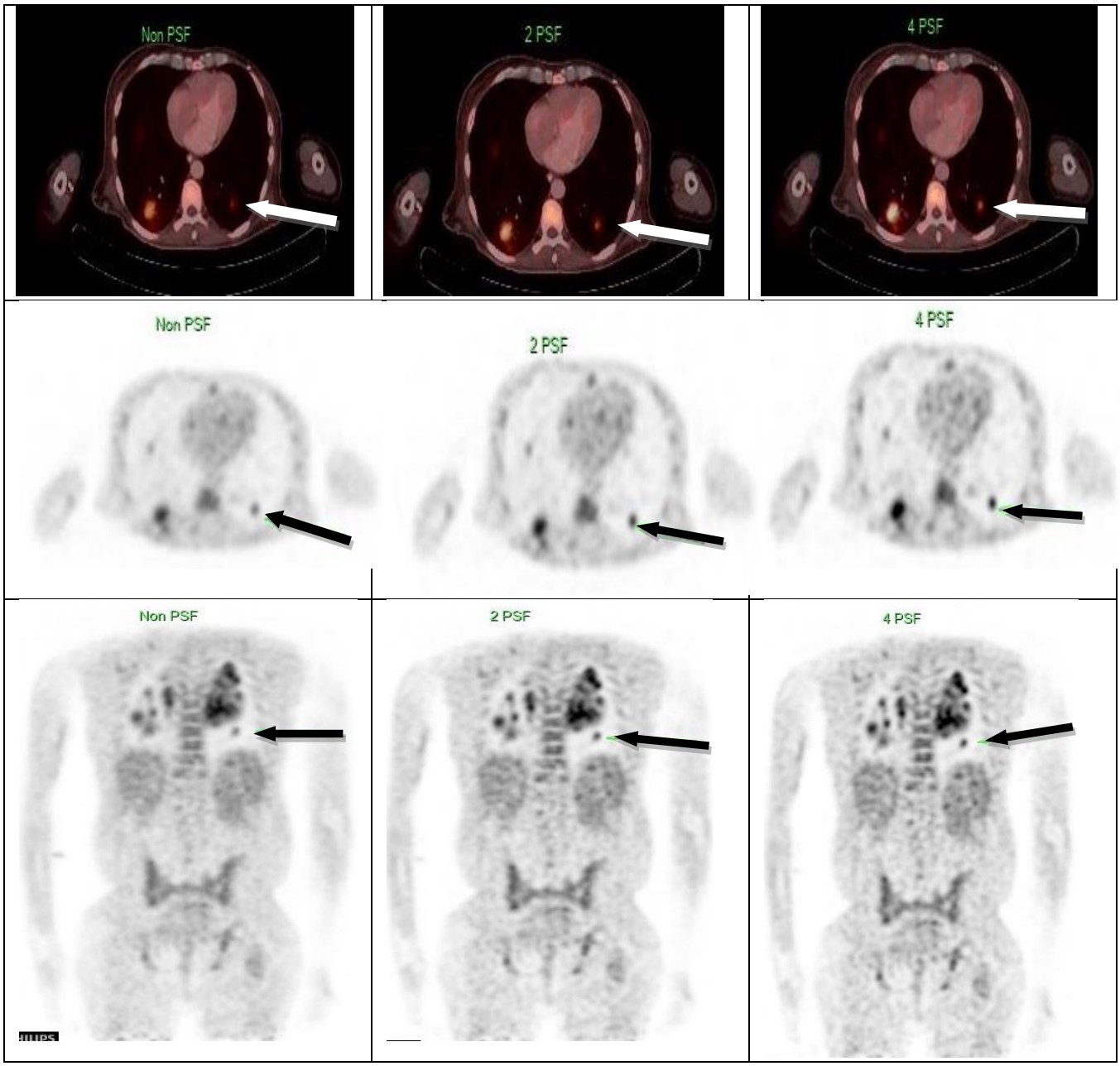

Fig. 3. Each column shows fused axial PET/CT, PET axial and PET coronal images in non PSF, 2 PSF and 4 PSF reconstruction. Top row- non PSF, 2PSF & 4PSF fused axial PET/CT images; Middle row- non PSF, 2PSF & 4PSF axial PET images and bottom row- non PSF, 2PSF & 4PSF coronal PET images. Arrow shows the lesion visibility in the different reconstructed images.